

Application of Inverse Techniques to Determine Heat-Transfer Coefficients in Heat-Treating Operations

B. Hernandez-Morales, J.K. Brimacombe, and E.B. Hawbolt

An existing sequential function specification algorithm for the solution of the inverse heat conduction problem (IHCP) has been applied to determine the response of both the surface heat flux and the surface temperature of flat stainless steel samples subjected to water quenching under controlled laboratory conditions that ensured one-dimensional heat flow. From this information, combined convective and radiative heat-transfer coefficients have been obtained as a function of steel surface temperature. The computer code was subsequently modified to solve the IHCP for air-cooled cylindrical carbon steel samples. In the algorithm, the problem is linearized by assuming the thermophysical properties of the steel to be fixed at values from the previous time step while estimating the current surface heat flux, which results in a more efficient code without a severe loss of accuracy. When compared with iterative ("brute force") methods commonly used in the past, techniques like sequential function specification offer a more robust strategy for solving the IHCP. By including information on future measurements, while solving for the unknown surface heat flux at a particular time, the sequential function specification algorithm effectively prevents over-responses to measured temperatures, and large variations in calculated heat-transfer coefficients, observed when sequential matching is applied, can be reduced. Sensitivity coefficients, a measure of the response of temperature to changes in the unknown surface heat flux which are calculated with this algorithm, can be used to design experiments involving the IHCP effectively.

1. Introduction

TRADITIONALLY, the processing conditions needed to produce the optimal heat treatment cycle for a particular metal part have been obtained through extensive empirical work, which is costly and does not provide information regarding the thermal and microstructural processes that take place during the operation. More recently, the coupling of transport phenomena and microstructural concepts, aided by the explosive growth of computational capabilities, has resulted in a more systematic approach to the designing of heat treating operations[1-3] and an explicit definition of operating parameters such as holding times and cooling conditions (water pressure, air velocity, nozzle design).

A critical aspect of this approach is the determination of heat-transfer conditions at the surface of the part to characterize the boundary condition, which typically involves a combined radiation and convection heat-transfer coefficient, usually defined in terms of surface temperature. To calculate the heat-transfer coefficient, both surface temperature and surface heat flux must be estimated; however, these variables are difficult to determine directly by experimental means. Instead, the procedure followed normally involves measurement of the temperature response inside the body, which is subsequently converted into heat flux and temperature at the surface. This is the inverse heat conduction problem (IHCP), which is schematically illustrated in Fig. 1 for the case of a one-dimensional single sensor. In the figure, the measured temperature at the sensor location is designated $Y(t)$, whereas the box outlined by the broken line at BC 2 emphasizes the fact that the boundary condition at $x = L$ is unknown. In this example, a boundary condition of symmetry ($\partial T/\partial x = 0$) is imposed at $x = 0$.

The IHCP is an ill-posed problem (as opposed to a well-posed heat conduction problem that satisfies the following criteria: existence, uniqueness, and stability of the solution) and

C_p	Heat capacity, J kg^{-1} K^{-1}
D	Rod diameter, mm
h	heat-transfer coefficient, W m^{-2} K^{-1}
J_0	Bessel function of the first kind of order zero, dimensionless
J_1	Bessel function of the first kind of order one, dimensionless
k	Thermal conductivity, W m^{-1} K^{-1}
L	Length of cylinder, mm
L	Plate half-thickness, mm
q	Surface heat flux, W m^{-2}
r	Radial coordinate, m
γ	Number of future time steps, dimensionless
R	Radius of cylinder, m
S	Least-squares function, °C^2
t	Time, s
T	Temperature, °C
T_f	Fluid temperature, °C
T_o	Initial temperature, °C
T_s	Surface temperature, °C
x	Axial coordinate, m
X	Sensitivity coefficient, °C W^{-1} m^2
Y	Measured temperature, °C
α	Thermal diffusivity, m^2 s^{-1}
ρ	Density, kg m^{-3}
Δt	Time step, s
$\wedge$	Denotes estimated quantity

B. Hernandez-Morales, J.K. Brimacombe, and **E.B. Hawbolt,** The Centre for Metallurgical Process Engineering, The University of British Columbia, Vancouver, Canada.

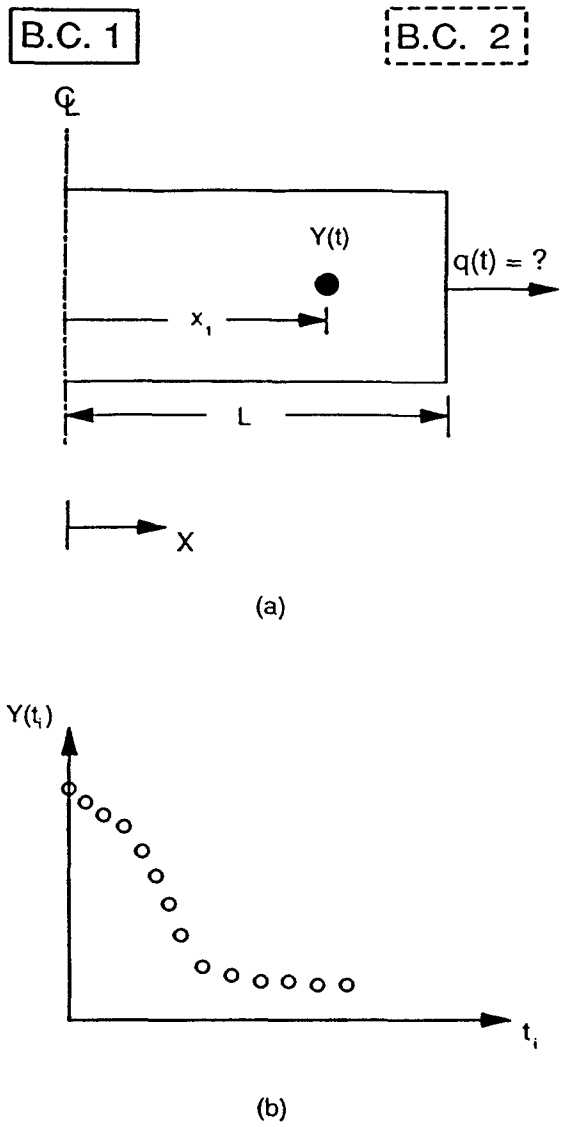

Fig. 1 (a) Schematic representation of a one-dimensional, single-sensor IHCP in a flat plate of thickness $2L$; the sensor is located at position x_1. The boundary conditions are as follows: $x = 0$, symmetry ($\partial T/\partial x = 0$); and at $x = L$, unknown time-dependent heat flux. (b) Discrete temperature measurements, $Y(t_i)$, at position x_1.

cannot be solved with the methods used for direct problems. Up to now, most of the IHCPs arising in metallurgical heat treating operations have been solved using a "brute force" method, in which a numerical scheme describing the direct heat conduction problem inside the part is solved iteratively for various guessed values of the surface heat flux until calculated temperature values correspond to those obtained via thermocouple measurements. A major disadvantage of this technique is that sequential matching of a single thermocouple (the most usual experimental configuration) is highly sensitive to measurement errors, particularly so as smaller time steps are used in solving the discretizing equations. A more robust approach can

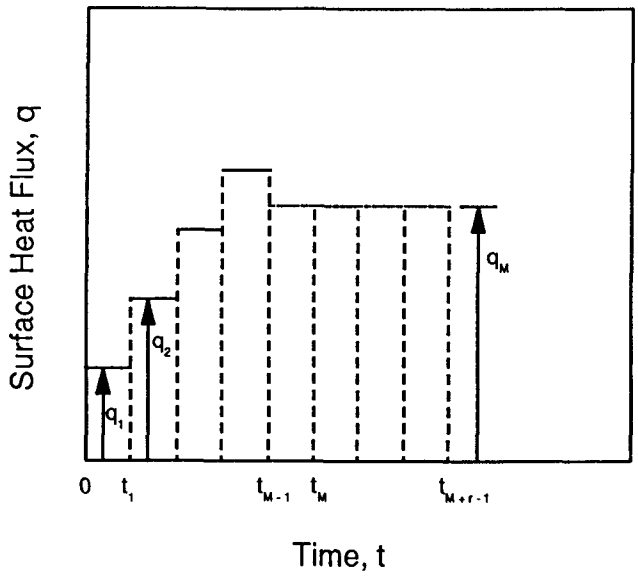

Fig. 2 Piecewise approximation of the surface heat flux as a function of time. The constant heat flux functional between t_{M-1} and t_{M+r-1} is adopted to calculate q^M in the sequential function specification algorithm.[4]

be obtained from a statistical treatment of the experimental data, which is presented in the following section.

2. IHCP Algorithm[4]

There are three basic methods to solve the IHCP problem—function specification, regularization, and mixed formulation (trial function method)—each of which can be implemented sequentially, *i.e.*, calculating a single component of the surface heat flux at a time, or for the whole time domain, where all components of the surface heat flux are computed simultaneously. The main advantage of a sequential algorithm is a major improvement in computing time. The algorithm adopted in this investigation was proposed by Beck *et al.*[4] and follows a sequential function specification approach, *i.e.*, a functional form is assumed for the unknown surface heat flux. In particular, the surface heat flux at each time step is estimated assuming it to be temporarily constant for a finite number of future time steps (see Fig. 2).

The unknown heat flux at the surface is obtained from temperature measurements including several future time steps by minimizing the following least-squares expression with respect to the heat flux component at time $t = t_M$, q^M:

$$S = \sum_{i=1}^{r} \sum_{j=1}^{J} \left(Y_j^{M+i-1} - T_j^{M+i-1} \right)^2 \qquad [1]$$

where Y_j^{M+i-1} is the measured temperature at the jth sensor at time t_{M+i-1}; T_j^{M+i-1} is the corresponding calculated temperature; and r is the number of future time steps adopted for estimating q^M.

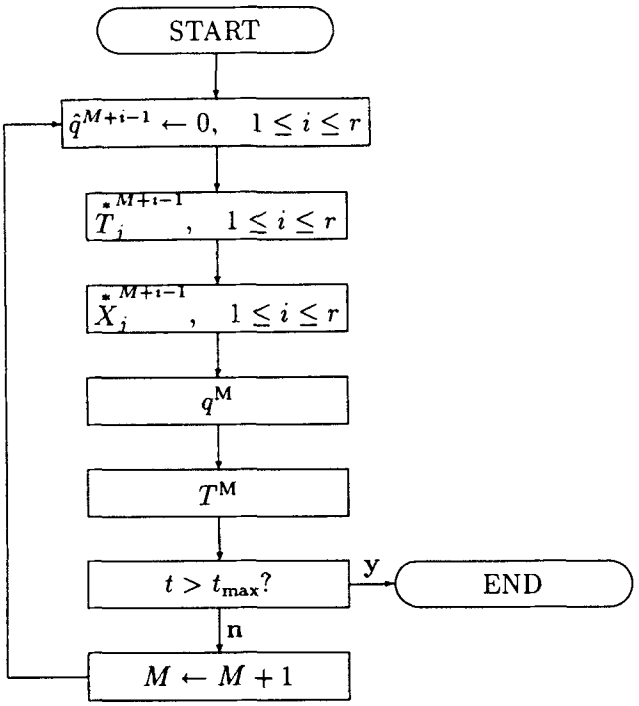

Fig. 3 Flowchart of the sequential function specification algorithm adopted for the solution of the IHCP.

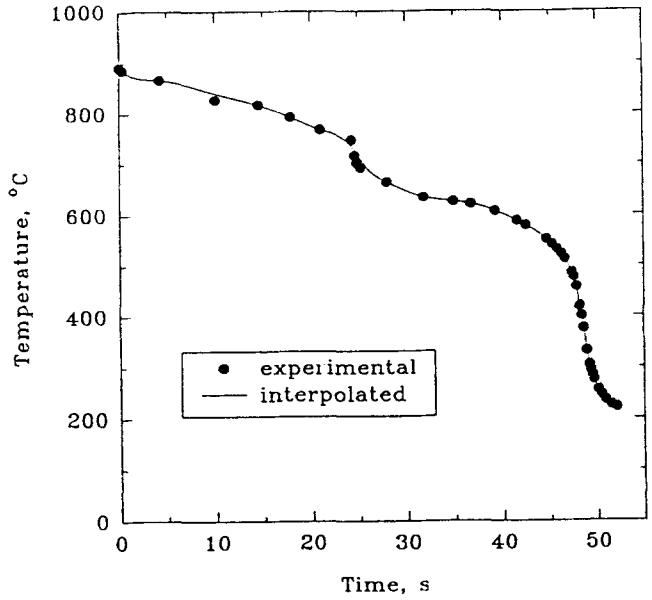

Fig. 4 Data input for the quenching problem. Closed circles are measured temperatures for a stainless steel disk quenched in still water at 60 °C[6]; the solid line is based on interpolated values used as input to the computer code.

Table 1 Thermal Conductivity (k) and Volumetric Heat Capacity (ρC_p) of Type 304 Stainless Steel[6]

T, °C	k, W m^{-1} K^{-1}	ρC_p, 10^6 J m^{-3} K^{-1}
50	15.9	4.0
250	17.6	4.27
500	21.8	4.70
550	23.02	4.88
750	26.4	4.82
800	26.8	4.87
850	26.4	4.86
900	26.8	4.83

Differentiating Eq 1 with respect to q^M, replacing q^M by $\hat{q}^M$ (the estimated heat flux at time t_M), and setting the expression equal to zero, one obtains:

$$2\sum_{i=1}^{r}\sum_{j=1}^{J}\left(Y_j^{M+i-1} - T_j^{M+i-1}\right)\left(\partial\frac{T_j^{M+i-1}}{\partial q^M}\right) = 0 \qquad [2]$$

with the equation evaluated at $\hat{q}^M$.

The future temperature at the sensor position j, T_j^{M+i-1}, can be calculated from a Taylor series expansion about $\hat{q}^{M-1}$:

$$T_j^{M+i-1} = T_j^{*M+i-1} + (q^M - \hat{q}^{M-1})X_j^{*M+i-1} \qquad [3]$$

where the asterisk implies that the T and X functions are evaluated using the thermal properties and surface heat flux values at time t_{M-1}. The quantity X_j^{M+i-1} is called the sensitivity coefficient and is defined by:

$$X_j^{M+i-1} = \frac{\partial T_j^{M+i-1}}{\partial q^M} \qquad [4]$$

Introducing Eq 3 into Eq 2 and solving for $\hat{q}^M$ gives:

$$\hat{q}^M = \hat{q}^{M-1} + \frac{1}{\Delta M}\sum_{i=1}^{r}\sum_{j=1}^{J}\left(Y_j^{M+i-1} - T_j^{*M+i-1}\right)X_j^{*M+i-1} \qquad [5]$$

where

$$\Delta M = \sum_{i=1}^{r}\sum_{j=1}^{J}\left(X_j^{*M+i-1}\right)^2 \qquad [6]$$

Note that by estimating $T^M \ldots T^{M+r-1}$ and $X^M \ldots X^{M+r-1}$ by adopting the thermophysical properties, k and ρC_p, which correspond to the previous time step, the problem has been linearized, and Eq 5 is explicit in q^M. The justification for this assumption is that, for a small time step, Δt, the thermal properties change little at a given location from one time to the next, even though there may be a large variation in properties from one end of the body to the other. An iterative procedure is then

not needed even for a problem with varying thermal properties. A flowchart for this algorithm is given in Fig. 3.

Once the response of the heat flux and temperature at the surface have been calculated, they are used to estimate the heat-transfer coefficient. It should be noted that the algorithm calculates $\hat{q}$ and $\hat{T}_s$, but they are calculated at slightly different times; $\hat{q}^M$ is best associated with $t_{M-1/2}$, whereas $\hat{T}_s$ corresponds to t_M. Therefore, the heat-transfer coefficient at time t_M is estimated from:

$$\hat{h}^M = \frac{\hat{q}^M + \hat{q}^{M+1}}{2\left(T_j^M - \hat{T}_S^M\right)} \qquad [7]$$

The computer program CONTA[5] incorporates the sequential function specification algorithm described above for a one-dimensional, planar IHCP, and is applied in the next section.

3. Application of IHCP Techniques to Heat-Treating Operations

Most metallurgical operations involve heat-transfer under conditions that make the direct experimental determination of heat-transfer coefficients very difficult, and therefore, the possibilities of applying the IHCP algorithms are virtually limitless. In this section, heat-transfer coefficients for quenching and air cooling under controlled laboratory conditions are calculated using the inverse algorithm described in the previous section. For the quenching example, the original CONTA code was used; however, for the controlled cooling of steel rod, a version of the code in cylindrical coordinates was developed.

3.1 *Quench Heat-Transfer Coefficients*

To determine the relationship between heat-transfer coefficient and surface temperature during quenching, Gupta[6] measured the thermal response at an inside location of heated disks (20 cm diameter, 2 cm thickness) immersed in brine, water, oil, and air. The disks were made of type 304 stainless steel.

Considering the ratio of diameter to thickness, the heat-transfer inside the specimen can be assumed to be one dimensional in cartesian coordinates. Because the specimen is fully immersed in the fluid, a symmetric temperature distribution about the mid-plane can be assumed, and the direct heat conduction problem is described by:

$$\frac{\partial}{\partial x}\left(k\frac{\partial T}{\partial x}\right) = \frac{\partial}{\partial t}(\rho C_p T) \qquad [8]$$

subject to the following boundary conditions (BC):

$$\text{BC 1: } \frac{\partial T}{\partial x} = 0 \qquad \text{at } x = 0 \text{ (symmetry)}$$

Table 2 Case 1 Constant Surface Heat Flux

$R = 5 \times 10^{-2}$ m
$\alpha = 0.00125\ \text{m}^2\,\text{s}^{-1}$
$q_o = 50\ \text{W m}^{-2}$
$k = 25\ \text{W m}^{-1}\,\text{K}^{-1}$
$C_p = 200\ \text{J kg}^{-1}\,\text{K}^{-1}$
$\rho = 100\ \text{kg m}^{-3}$

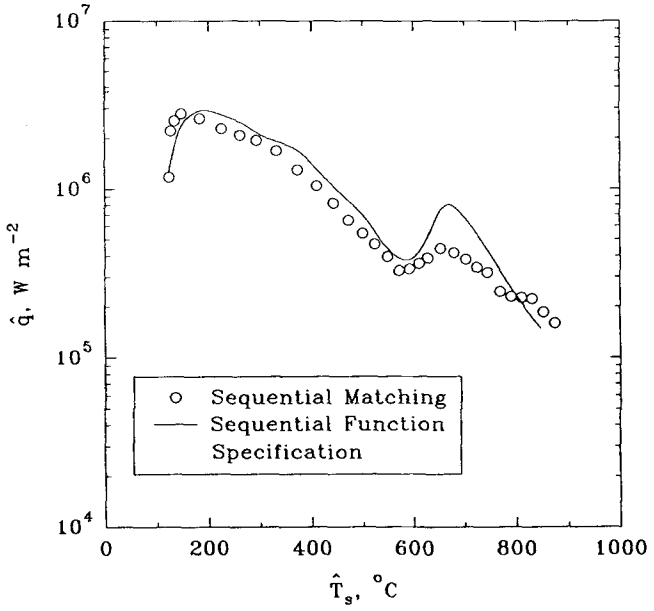

Fig. 5 Estimated surface heat flux as calculated by Gupta[6] (open circles) and from this work (solid line) for the quenching of a stainless steel disk in still water at 60 °C.

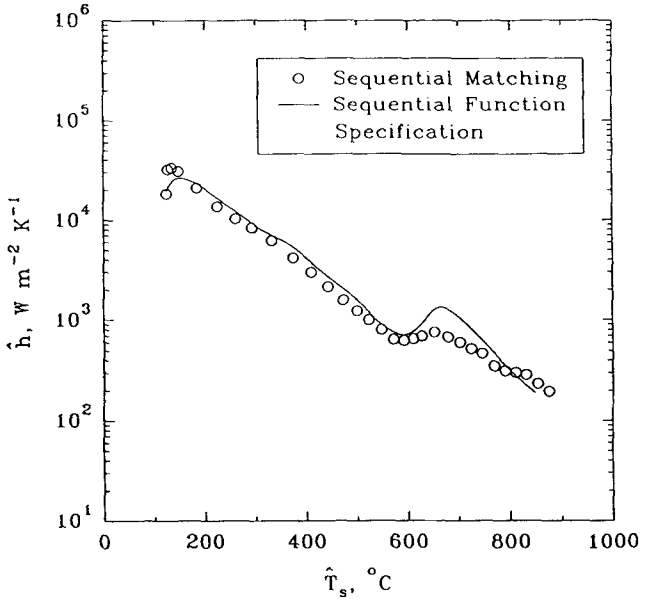

Fig. 6 Estimated heat-transfer coefficient as calculated by Gupta[6] (open circles) and from this work (solid line) for the quenching of a stainless steel disk in still water at 60 °C.

$$\text{BC 2: } -k\frac{\partial T}{\partial x} = -\bar{h}(T_f - T) \qquad \text{at } x = L/2 \text{ (convection)}$$

where $T = T(x,t)$ and L is the thickness of the disk.

The computer program CONTA was applied to measurements obtained on the type 304 stainless steel disk quenched in still water at 60 °C with a thermocouple located 1.4 mm from the surface. The thermophysical properties of the stainless steel are summarized in Table 1.

For calculation purposes, the specimen was subdivided into two regions of 1.4 mm (6 nodes) and 9.35 mm (14 nodes), respectively. The temperature response adopted as input to the program was obtained by interpolation of the experimental measurements, as shown in Fig. 4. Note that CONTA requires the input data at equally spaced times, but they need not coincide with the experimental times. The calculational time interval adopted, Δt, was 0.0625 s for two future time steps ($r = 2$).

The estimated heat flux and heat-transfer coefficient, as a function of surface temperature, are shown in Fig. 5 and 6. Good agreement between the estimates of this study based on the sequential function specification algorithm and those obtained by adopting a sequential matching approach[6] can be seen. Estimated heat-transfer coefficients as a function of estimated surface temperature, obtained using the sequential function specification technique, for a variety of quenching conditions have been reported elsewhere.[7]

3.2 *Controlled Cooling of Steel Wire Rod*

Campbell *et al.*[8] measured the thermal response at the centreline of rods during forced air cooling. The experiments involved a range of steel grades, rod diameters, and air velocities and were designed to simulate the Stelmor process. The specimens were long cylinders ($L/D > 25$). Therefore, a mathematical description of the problem is given by:

$$\frac{1}{r}\frac{\partial}{\partial r}\left(kr\frac{\partial T}{\partial r}\right) = \frac{\partial}{\partial t}(\rho C_p T) \qquad [9]$$

subject to the following boundary conditions:

$$\text{BC 1: } \frac{\partial T}{\partial r} = 0 \qquad \text{at } r = 0 \text{ (symmetry)}$$

$$\text{BC 2: } -k\frac{\partial T}{\partial r} = -\bar{h}(T_f - T) \qquad \text{at } r = R \text{ (convection)}$$

where $T = T(r,t)$.

Accordingly, the original computer code CONTA was modified to accommodate cylindrical coordinates. Once coded and debugged, the program was tested by comparing results obtained using analytical solutions for two cases: (1) a solid cylinder subjected to a constant surface heat flux and (2) a solid cylinder subjected to a medium of constant heat-transfer coefficient and fluid temperature. In both cases, the direct problem was first solved analytically to obtain the thermal response at a given point in the domain, which was then adopted as input to the numerical solution of the IHCP to estimate both surface heat flux and surface temperature.

3.2.1 *Case 1: Solid Cylinder Subjected to a Constant Heat Flux at the Surface*

This problem is described mathematically by Eq 9 (assuming constant thermophysical properties), subject to the following boundary and initial conditions:

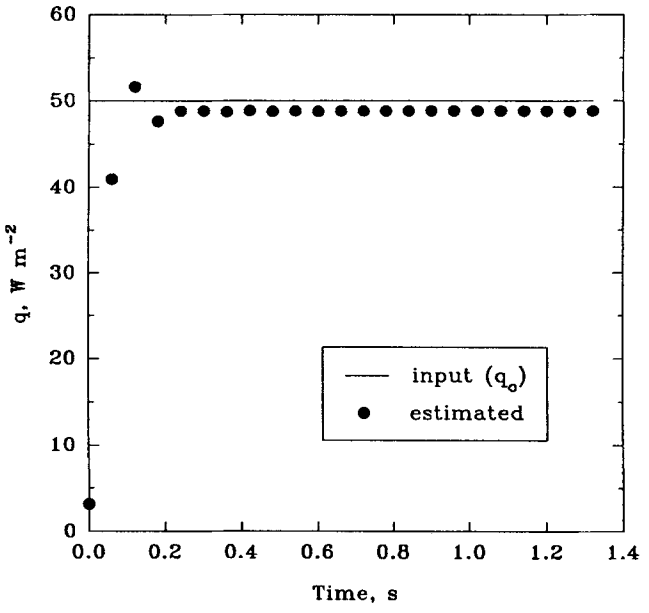

Fig. 7 Estimated and true surface heat flux for Case 1, constant surface heat flux.

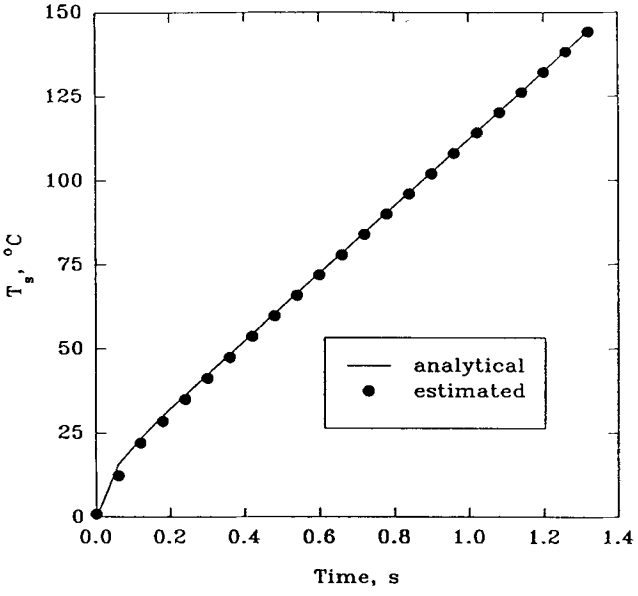

Fig. 8 Estimated, using the sequential function specification technique, and analytical thermal response at the surface of the cylinder for Case 1, constant heat flux.

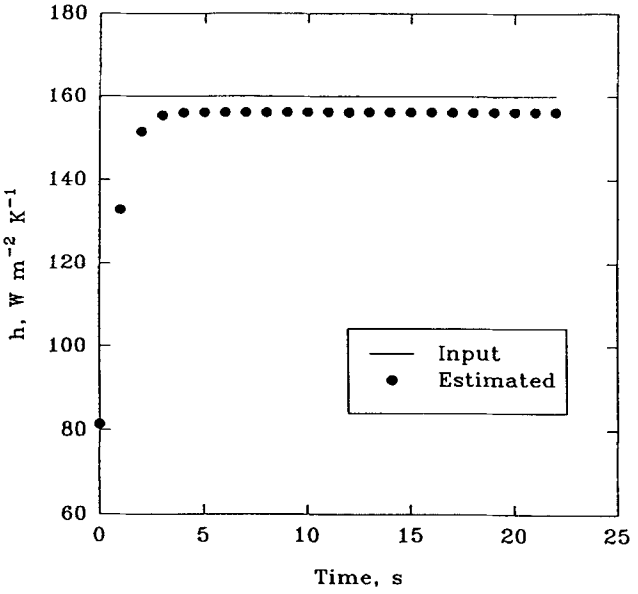

Fig. 9 Estimated and true heat-transfer coefficient for Case 2, constant heat-transfer coefficient.

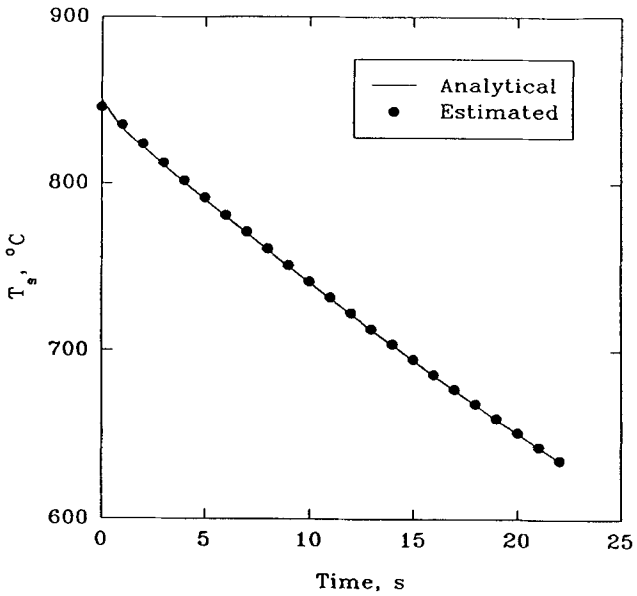

Fig. 10 Estimated, using the sequential function specification technique, and analytical thermal response at the surface of the cylinder for Case 2, constant heat-transfer coefficient.

Table 3 Case 2 Constant Heat-Transfer Coefficient

$h = 160\ \mathrm{W\,m^{-2}\,K^{-1}}$
$T_f = 20\ ^\circ\mathrm{C}$
$T_o = 850\ ^\circ\mathrm{C}$
$R = 5\ \mathrm{mm}$
$k = 25\ \mathrm{W\,m^{-1}\,K^{-1}}$
$C_p = 625\ \mathrm{W\,m^{-1}\,K^{-1}}$
$\rho = 7650\ \mathrm{kg\,m^{-3}}$

$$\text{BC 1: } \frac{\partial T}{\partial r} = 0 \qquad \text{at } r = 0 \text{ (symmetry)}$$

$$\text{BC 2: } -k\frac{\partial T}{\partial r} = q_o \qquad \text{at } r = R \text{ (prescribed heat flux)}$$

$$\text{IC: } T(r,0) = T_o$$

for which an analytical solution, for $T_o = 0$, is available:[9]

$$T(r,t) = \frac{2q_o\alpha t}{kR} + \frac{q_o R}{k}\left\{\frac{r^2}{2R^2} - \frac{1}{4} - 2\sum_{n=1}^{\infty}\exp\left(\frac{-\alpha\beta_n^2 t}{R^2}\right)\frac{J_o(r\beta_n/R)}{\beta_n^2 J_0(\beta_n)}\right\} \quad [10]$$

where β_n are the roots of the transcendental equation

$$J_1(\beta_n) = 0 \quad [11]$$

The results at the centreline, $T(0,t)$, were used as input for the program, and the surface heat flux was recalculated. Figure 7 shows a plot of estimated surface heat flux versus time as well as the true heat flux (the value used to calculate T (0, t) in Eq 14); good agreement can be observed, except at early times. The thermal response at the surface was also computed and compared to the analytical solution; very good agreement can be seen, as shown in Fig. 8.

Table 4 Chemical Composition of Steel Used for Controlled Air Cooling Tests

Element	wt%
Carbon	0.69
Manganese	0.76
Phosphorus	0.014
Sulfur	0.019
Silicon	0.22
Copper	0.008
Nickel	0.005
Chromium	0.028
Molybdenum	0.002
Vanadium	0.002
Niobium	0.002

3.2.2 *Case 2: Solid Cylinder Subjected to a Medium of Constant Heat-Transfer Coefficient*

Assuming constant thermal properties, this problem can be described by Eq 9 subject to:

$$\text{BC 1: } \frac{\partial T}{\partial r} = 0 \qquad \text{at } r = 0 \text{ (symmetry)}$$

$$\text{BC 2: } -k\frac{\partial T}{\partial r} = -\bar{h}(T_a - T) \qquad \text{at } r = R \text{ (convection)}$$

$$\text{IC: } T(r,0) = T_o$$

The analytical solution is given in Ref 10 as:

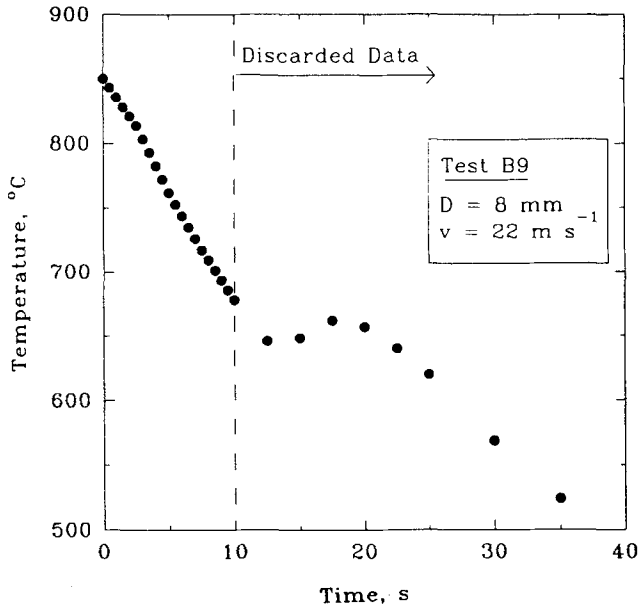

Fig. 11 Data input for cooling of a 8-mm diam carbon steel rod in air flowing at 22 m s^{-1}.[8]

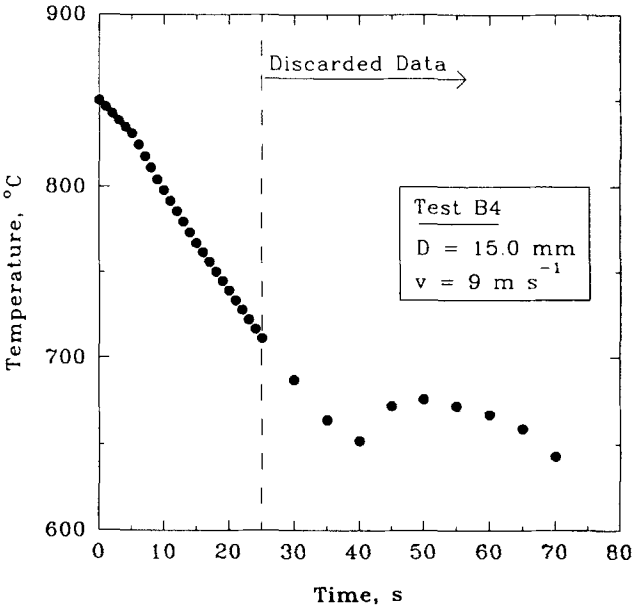

Fig. 12 Data input for cooling of a 15-mm diam carbon steel rod in air flowing at 9 m s^{-1}.[8]

$$T(r,t) = \frac{2HT_o}{R} \sum_{m=1}^{\infty} \frac{J_o(\beta_m r)}{(\beta_m^2 + H^2) J_o(\beta_m R)} \exp(-\alpha\beta_m^2 t) \qquad [12]$$

where $H = \bar{h}/k$.

The program was run taking the thermal response at the centreline calculated with the analytical solution as input, and the heat-transfer coefficient was back-calculated. Figure 9 shows

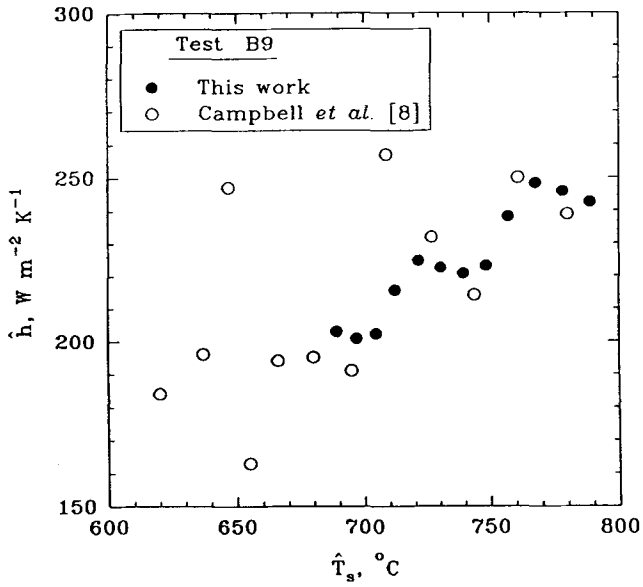

Fig. 13 Estimated heat-transfer coefficient for air cooling (test B9) calculated by Campbell *et al.*[8] (open circles) and in this work (closed circles).

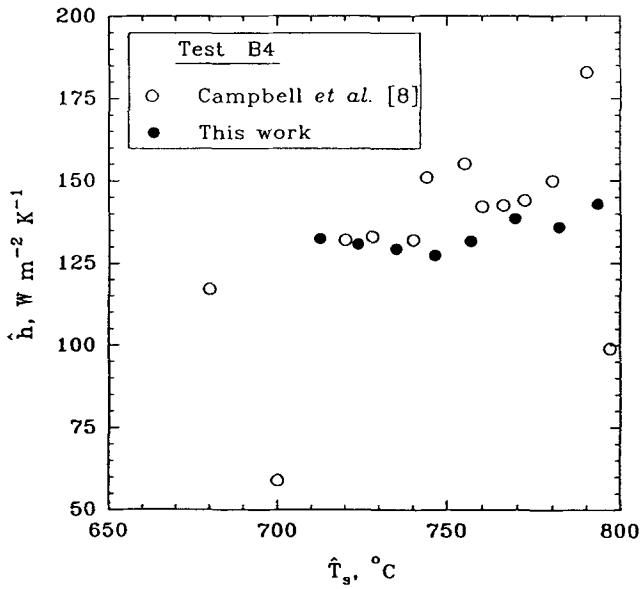

Fig. 14 Estimated heat-transfer coefficient for air cooling (test B4) calculated by Campbell *et al.*[8] (open circles) and in this work (closed circles).

good agreement between estimated and true heat-transfer coefficients, except at early times. The estimated thermal response at the surface also agrees well with the analytical solution (Fig. 10). The data used are shown in Table 3.

The computer program was run for two experimental runs reported by Campbell *et al.*—run B9 (8-mm diam, cooled at 22 m/s) and run B4 (15-mm diam rod, cooled at 9 m/s); the steel composition is given in Table 4. The experimentally deter-

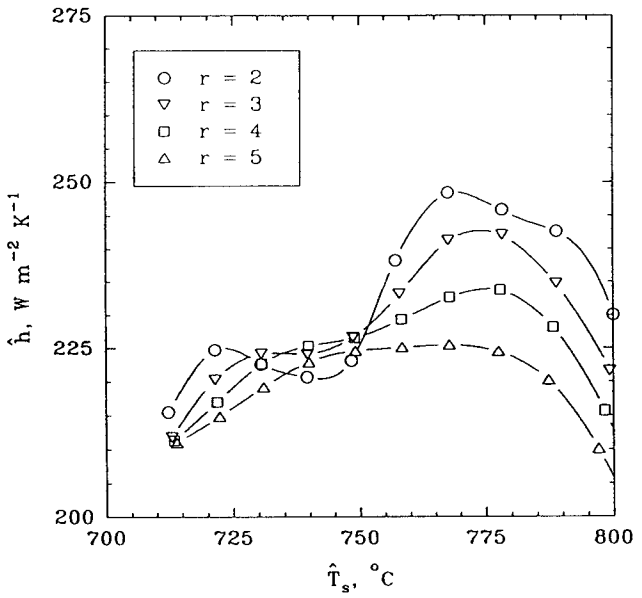

Fig. 15 Effect of number of future time steps, r, on the estimated heat-transfer coefficient. Input data taken from Fig. 11.

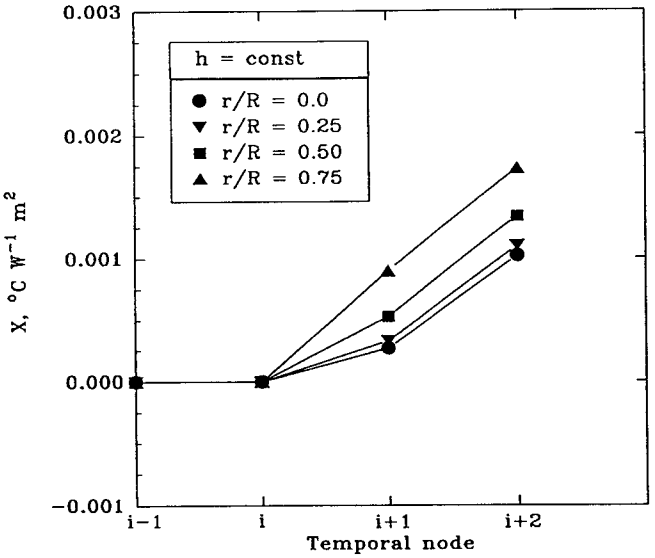

Fig. 16 Sensitivity coefficients at several radial positions in a solid cylinder subjected to a medium of constant heat-transfer coefficient and fluid temperature.

Table 5 Thermal Conductivity of Austenite in a Eutectoid Steel[8]

T, °C	k, W m^{-1} K^{-1}
650	21.5
700	22.2
750	23.0
800	23.8
850	24.7

Table 6 Volumetric Heat Capacity (ρC_p) of Austenite in a Eutectoid Steel[8]

T, °C	ρC_p, 10^6 J m^{-3} K^{-1}
650	4.44
676	4.45
725	4.48
775	4.57
830	4.64
875	4.73

mined thermal response at the centreline is shown in Fig. 11 and 12, respectively. It should be noted that only data that did not involve phase transformation were used. In this work, thermophysical data for a eutectoid plain-carbon steel were assumed for the experimental runs and are given in Tables 5 and 6.[8]

A total of 21 and 26 pairs of data points, $T(0,t)$, were obtained from the experimental curves of tests B9 and B4, respectively. The steel rod was discretized into 20 nodes, and a computational time step of 0.25 s was used for a value of $r = 2$.

The estimated heat-transfer coefficient as a function of computed steel surface temperature for tests B4 and B9 is shown in Fig. 13 and 14, respectively, together with results obtained by Campbell *et al.*,[8] using an iterative procedure based on an implicit finite-difference approximation of the direct problem. Good agreement can be seen, although it is important to note that calculations based on the sequential function specification exhibit less scatter.

The number of future time steps adopted for the calculation of the heat flux in Eq 5 is controlled by the parameter r. Figure 15 shows estimated heat-transfer coefficients obtained for values of $r = 2$, 3, 4, and 5; the data input was taken from test B9. As more information regarding future temperatures is considered (larger values of r), deviations in the values of $\hat{h}$ are attenuated. This is a key feature of the sequential function specification algorithm and results in an efficient code that overcomes the extreme sensitivity to measurement errors normally associated with the IHCP. In contrast, algorithms based on matching calculated to measured temperature responses on a one-to-one basis exhibit large deviations.

The sensitivity coefficients, X_j, which are calculated as part of the solution to the IHCP, represent a quantitative measure of the sensitivity of the thermal response to changes in the unknown surface heat flux (see Eq 4) and can, therefore, be used to design experiments. In general, one is interested in large, uncorrelated values of X_j, which means that more nonrepetitive information can be extracted from the experimentally determined thermal response. Figure 16 shows calculated sensitivity coefficients at several positions across the radius of a solid cylinder subjected to a constant heat-transfer coefficient and fluid temperature. It can be seen that the largest values of the sensitivity coefficient occur at the position closest to the surface of the cylinder; the implication of this result is that every effort should be made to place the thermocouples as close to the surface as practicably possible. Lambert and Economopoulos[11] established a linear relationship between the logarithm of the mean error of the determined heat-transfer coefficient and the distance of the point of measurement below the surface for cy-

lindrical samples. They showed a value of the mean error as high as 10% for a position 2 mm below the surface, then dropping to less than 1% for a measurement taken 1 mm below the surface when long cylinders of 20-mm diam were used.

4. Conclusions

Heat-transfer coefficients for the simulation of two heat-treating operations carried out under controlled laboratory conditions have been obtained using an existing sequential function specification algorithm to solve the IHCP. For the solution of the IHCP in flat specimens quenched in still water, the original computer program was used, whereas to obtain heat-transfer coefficients under conditions that simulate the Stelmor process, the code was modified to include cylindrical coordinates.

Inverse techniques like sequential function specification are more fundamentally based than the previously used iterative approach (one sensor, exact matching), thus eliminating the need for guessing values of surface heat flux; they also allow linearization of the problem, which results in highly efficient codes. The results obtained in this investigation exhibited less scatter in the values of the estimated heat-transfer coefficient compared to those obtained via iterative (brute force) algorithms.

When the number of future time measurements considered for the calculations is increased (larger values of r), over-responses to sudden changes in the experimentally determined temperature response, which might be associated to measurement errors, are damped. Therefore, the sequential function specification algorithm minimizes one of the main concerns regarding the IHCP.

Sensitivity coefficients, which are the derivative of the thermal response with respect to the unknown surface heat flux calculated as part of the sequential function specification algorithm, can be used to optimize experimental design. In this work, it was shown that, by locating the sensor as close to the surface of a solid cylinder as possible, higher values of sensitivity coefficients were obtained, and therefore, more information could be extracted.

Acknowledgments

The authors are grateful to the Natural Sciences and Engineering Council of Canada for financial support of this study. The assistance of Prof. J.V. Beck (Michigan State University) in providing the original code CONTA is gratefully acknowledged. One of the authors (B. Hernandez-Morales) is also grateful for the financial support provided by Universidad Nacional Autónoma de México. Discussions with Mr. Fernando Medina were very helpful.

References

1. F.M.B. Fernandez, S. Denis, and A. Simon, Mathematical Model Coupling Phase Transformation and Temperature Evolution During Quenching of Steels, *Mater. Sci. Technol.*, Vol 1 (No. 10), 1985, p 838-844.
2. S. Sjöström, Interactions and Constitutive Models for Calculating Quench Stresses in Steel, *Mater. Sci. Technol.*, Vol 1 (No. 10), 1985, p 823-829.
3. B. Hildenwall and T. Ericsson, Prediction of Residual Stresses in Case-Hardening Steels, in *Hardenability Concepts with Applications to Steel*, D.V. Doane and J.S. Kirkaldy, Ed., The Metallurgical Society of AIME, 1978, p 579-606.
4. J.V. Beck, B. Litkouhi, and C.R. St. Clair, Jr., Efficient Sequential Solution of the Nonlinear Inverse Heat Conduction Problem, *Numerical Heat Transfer*, Vol 5, 1982, p 275-286.
5. J.V. Beck, "User's Manual for CONTA—Program for Calculating Surface Heat Fluxes From Transient Temperatures Inside Solids," Sandia National Laboratory, Report SAND83-7134, Dec 1983.
6. S.M. Gupta, M.A.Sc thesis, University of British Columbia, 1977.
7. B. Hernandez-Morales, S.M. Gupta, J.K. Brimacombe, and E.B. Hawbolt, Determination of Quench Heat-Transfer Coefficients Using Inverse Techniques, in *1st Int. Conf. Quenching and Control of Distortion*, ASM International, Sept 1992.
8. P.C. Campbell, E.B. Hawbolt, and J.K. Brimacombe, Microstructural Engineering Applied to the Controlled Cooling of Steel Wire Rod: Part I. Experimental Design and Heat Transfer, *Metall. Trans. A*, Vol 22, 1991, p 2769-2778.
9. H.S. Carslaw, *Conduction of Heat in Solids*, 2nd ed., Clarendon Press, Oxford, 1959, p 203.
10. M. Necati Özisik, *Heat Conduction*, John Wiley & Sons, 1980, p 101-102.
11. N. Lambert and M. Economopoulos, Measurement of the Heat-Transfer Coefficients in Metallurgical Processes, *JISI*, Vol 208 (No. 10), 1970, p 917-928.